Geophysical Research Letters®

RESEARCH LETTER
10.1029/2022GL099574

On the Role of Rheological Memory for Convection-Driven Plate Reorganizations

L. Fuchs[1] and T. W. Becker[2,3,4]

[1]Institute for Geosciences, Goethe University, Frankfurt/Main, Germany, [2]Jackson School of Geosciences, Institute for Geophysics, The University of Texas at Austin, Austin, TX, USA, [3]Department of Geological Sciences, Jackson School of Geoscience, The University of Texas at Austin, Austin, TX, USA, [4]Oden Institute for Computational Engineering and Sciences, The University of Texas at Austin, Austin, TX, USA

Key Points:

- Results from global, plate-generating convection models with damage
- Self-consistently formed persistent weak zones lead to more frequent plate reorganizations
- Accumulation of weak zones might counteract decrease in convective vigor for tectonic variability

Supporting Information:

Supporting Information may be found in the online version of this article.

Correspondence to:

L. Fuchs,
fuchs@geophysik.uni-frankfurt.de

Citation:

Fuchs, L., & Becker, T. W. (2022). On the role of rheological memory for convection-driven plate reorganizations. *Geophysical Research Letters*, *49*, e2022GL099574. https://doi.org/10.1029/2022GL099574

Received 16 MAY 2022
Accepted 1 SEP 2022

Abstract Understanding the temporal variability of plate tectonics is key to unraveling how mantle convection transports heat, and one critical factor for the formation and evolution of plate boundaries is rheological "memory," that is, the persistence of weak zones. Here, we analyze the impact of such damage memory in global, oceanic-lithosphere-only models of visco-plastic mantle convection. Self-consistently-formed weak zones are found to be reactivated in distinct ways, and convection preferentially selects such damaged zones for new plate boundaries. Reactivation of damage zones increases the frequency of plate reorganizations, and hence reduces the dominant periods of surface heat loss. The inheritance of distributed lithospheric damage thus dominates global surface dynamics over any local boundary stabilizing effects of weakening. In nature, progressive generation of weak zones may thus counteract and perhaps overcome any effects of reduced convective vigor throughout planetary cooling, with implications for the frequency of orogeny and convective transport throughout Wilson cycles.

Plain Language Summary Understanding how and why the motion of the lithosphere changes over time is important since this is telling us how planets with a plate tectonic style of heat transport evolve by thermo-chemical mantle convection. One important factor for the evolution of plate boundaries is hysteresis, that is, memory of past deformation. Inherited weak zones, such as sutures, and progressive weakening are well documented in the geological record. Convection with damage shows dynamical behavior that is different from pure plastic failure without memory, or homogenous lithosphere that is being newly broken. We analyze the impact of damage with global, oceanic-lithosphere-only models of plate-like mantle convection. Weak zones that are formed in an initially homogenous material are found to be reactivated subsequently in distinct ways. Within our tectonic system model, convection preferentially selects pre-damaged zones for new, active plate boundaries. This reactivation increases the frequency of plate reorganizations compared to models without damage, and also changes the time-dependence of cyclic surface heat loss. In nature, the progressive generation of weak zones over planetary history may counteract and perhaps overcome any effects of reduced convective vigor during cooling. This has implications for the frequency of mountain building and understanding Wilson cycles.

1. Introduction

Within our solar system, the style of plate tectonics on Earth is unique and key for the thermal evolution of our planet. The motions and reorganization of oceanic plates are part of the cold, surface boundary layer of mantle convection (Turcotte & Oxburgh, 1967), and embedded within are the creation and recycling of continents throughout the supercontinental cycle (e.g., Wilson, 1966). However, how the interactions between oceanic and continental systems serve to control the long-term trends and fluctuations of tectonic activity and heat transport remains debated (e.g., Condie et al., 2015; Mitchell et al., 2021; Zhong et al., 2007).

To form plate boundaries, high lithospheric strength as expected from temperature-dependent viscosity needs to be overcome (e.g., Moresi and Solomatov, 1998), and plastic yielding produces broadly plate-like surface planforms in global convection models (e.g., Foley and Becker, 2009; van Heck and Tackley, 2008). However, such models typically require yield stresses that are low compared to expectations from rock mechanics. Moreover, one possibly important ingredient, the weakening memory of past deformation, has largely been missing from global convection models. It is this memory effect of tectonic damage on which we focus here.

Supercontinental assembly and break-up through multiple Wilson cycles leave behind a heterogeneous lithosphere which can sustain weakened regions for perhaps longer than 10^9 years (e.g., Buiter & Torsvik, 2014; Burke et al., 1977; Sykes, 1978). Such weak zones, or damage zones, significantly differ from the surrounding lithosphere, for example, compositionally or mechanically, for example, due to failed rifts. Weak zones thus represent rheological "memory" which can be recalled, for example, for subduction initiation (e.g., Crameri et al., 2020; Gurnis et al., 2000) or supercontinental breakup (e.g., Dang et al., 2020). Given that continental plates record geology for ∼10 times longer than the more rapidly recycled oceanic lithosphere, memory effects may thus be most important for continents.

However, even if the lithosphere were purely oceanic, memory still matters, for example, because the formation of plate boundaries is connected to the processes reducing brittle or plastic strength with sustained deformation in the first place, that is, strain weakening and localization. While sphericity and high convective vigor appear to produce ridge offsets for visco-plastic convection (Langemeyer et al., 2021), it is typically held that deformation-dependent strength is required to explain hallmarks of plate tectonics (e.g., Bercovici, 1993; Gerya, 2013; Landuyt et al., 2008). Which micro-physical mechanisms serve to localize deformation (e.g., Montési, 2013) and if an isotropic description is sufficient (e.g., Tommasi & Vauchez, 2001) have long been debated, and there are numerous numerical explorations of different weakening formulations in 2-D and 3-D Cartesian convection models (e.g., Foley and Bercovici, 2014; Fuchs & Becker, 2019; Landuyt et al., 2008; Ogawa, 2003; Tackley, 2000a). Grain-size-dependent rheologies appear promising candidates for plate boundary evolution (e.g., Bercovici & Ricard, 2016), and the controls on damage creation and healing have far-reaching implications for planetary evolution (e.g., Foley and Bercovici, 2014; Foley and Driscoll, 2016).

Simplified descriptions based on tracking an evolving damage variable can capture much of the more complex hysteresis due to grain-size dependence (Fuchs & Becker, 2021), and such approximations are more readily explored within convection models (e.g., Ogawa, 2003; Tackley, 2000a). Here, we build on a range of earlier 2-D modeling and explore, to our knowledge for the first time, the effects of memory on global, visco-plastic convection. While we explore an idealized, oceanic plate only system at reduced convective vigor compared to Earth, for simplicity, interesting behavior arises that allows us to speculate on the role of damage for plate tectonics.

2. Methods

2.1. Model Setup

All computations were performed in a spherical shell using *CitcomS* (Moresi and Solomatov, 1995; Tan et al., 2006; Zhong et al., 2000), a well-benchmarked finite element code that solves the equations for conservation of mass, momentum, and energy in a fluid under the Boussinesq approximation:

$$u_{i,j} = 0 \tag{1}$$

$$-P_{,i} + (\eta u_{i,j} + \eta u_{j,i})_{,j} + RaT\delta_{ir} = 0 \tag{2}$$

$$T_{,t} + u_i T_{,i} = T_{ii} + H_T \tag{3}$$

Here u is velocity, P dynamic pressure, η viscosity, T temperature, and H_T internal heat production. The term $X_{,y}$ stands for the derivative of X in the direction of y, where i and j are the spatial indices, r is the radial direction, and t represents time (e.g., Zhong et al., 2000). The system is heated purely internally with a constant rate of non-dimensionalized heat production ($H_T = 60$, which scales to ∼7 TW), where we assume zero heat flux and free slip at the bottom and a constant temperature ($T = 0$) and free slip at the top. Pure internal heating excludes plumes as sources of plate reorganization (e.g., Arnould et al., 2020; Foley and Becker, 2009), again for simplicity. All parameters and scalings are summarized in Table S1 in Supporting Information S1. The effective Rayleigh number is $\sim 10^7$ based on a mantle depth scaling, about ∼a factor 100 below Earth's expected convective vigor at present-day (see Text S1 in Supporting Information S1 for more details).

2.2. Rheology

The temperature-dependence of viscosity is described by an Arrhenius-type relationship (e.g., Tackley, 2000b, 2000c) for the non-dimensional viscosity

$$\eta_T = \exp\left(\frac{\eta_e}{T+1} - \frac{\eta_e}{2}\right) \tag{4}$$

where η_e is the non-dimensional activation energy (23.03). Our parameters result in a total viscosity variation of 5 orders of magnitude providing a moderate viscosity contrast with respect to what is expected for Earth. However, visco-plastic convection with such viscosity ranges results in plate-like surface motions (e.g., Foley and Becker, 2009; van Heck and Tackley, 2008). While our models are thus not quite Earth-like, we consider them meaningful as a reference from which we explore the role of strain-dependent weakening and hardening (SDWH).

The strength of the material is defined by its yield stress (e.g., Tackley, 2000a, 2000c):

$$\sigma_y = \min(a + bz, \lambda) \tag{5}$$

where a is the cohesion, z depth, and b a gradient which approximates a normal stress dependent failure envelope for "brittle" behavior at shallow depths, and λ is a constant yield stress for deeper, "ductile" plasticity.

A simplified SDWH rheology can capture aspects of damage memory within the upper thermal boundary layer (TBL) of thermal convection (e.g., Fuchs & Becker, 2019, 2021). We explore the temporal evolution of a quasi-strain, γ, that plays the role of a damage variable as (e.g., Gerya, 2013; Ogawa, 2003; Tackley, 2000c):

$$\frac{d\gamma}{dt} = \dot{\varepsilon}_{II} - \gamma(t)H(T) \tag{6}$$

where $\dot{\varepsilon}_{II}$ is the second invariant of the strain rate tensor and H the temperature-dependent healing rate defined as (e.g., Tackley, 2000c):

$$H(T) = B\exp\left[\frac{-\eta_\gamma}{2}\left(\frac{1}{T+1} - \frac{1}{2}\right)\right] \tag{7}$$

Here, B is the healing time scale and η_γ a nondimensional activation energy. For a high (low) η_γ the healing term depends more (less) on temperature, and B governs the hardening rate within the mantle (e.g., Fuchs & Becker, 2019). This somewhat *ad-hoc* description can be viewed as an abstraction and constraint on the actual micro-physics (cf. Foley and Bercovici, 2014). As discussed by Fuchs and Becker (2021), we choose values for B and η_γ which result in similar (and slower) hardening rates compared to a single mineral phase, composite, grain-size-sensitive (GSS) rheology (cf. Hirth & Kohlstedt, 2003; Behn et al., 2009; Foley and Bercovici, 2014; see Text S2 in Supporting Information S1 for more details).

Different combinations of SDWH have been proposed. Here, we assume that a linear reduction of the yield stress due to γ, that is, plastic-strain softening, results in rheological weakening. Plastic-strain softening best approximates the transient weakening and hardening behavior of a GSS, composite rheology (Fuchs & Becker, 2021). While we limit the rheological weakening and hardening rates to the transient behavior of GSS rheology, additional microphysical mechanisms might be used as further constraints.

The effective yield stress is defined as (e.g., Lavier et al., 2000):

$$\tilde{\sigma}_y(t) = \sigma_y\left[1 - D_{\max}\frac{\gamma(t)}{\gamma_{cr}}\right] \tag{8}$$

where $D_{\max}$ (0.9) is the maximum damage and γ_{cr} (10) is the critical strain for which maximum damage is reached. The amplitude of γ governs the intensity of weakening, while healing leads to rheological hardening due to the increase of the yield stress. The yield and effective viscosity are then defined as (e.g., Tackley, 2000b, 2000c):

$$\tilde{\eta}_y = \frac{\tilde{\sigma}_y}{2\dot{\varepsilon}_{II}} \tag{9}$$

$$\eta_{eff} = \min\left(\eta_T, \tilde{\eta}_y\right) \tag{10}$$

2.3. Modeling Approach and Diagnostics

For our reference model without SDWH (marked as diamond in Figure 2), we chose a Rayleigh number, yield stress, and yield stress depth-gradient close to the transition to episodic-lid convection (cf. Foley and Becker, 2009) and subsequently increase the yield stress and its gradient. Our parameter combination leads to the most plate-like character (for our assumptions), that is, strong subducting slabs, and no yielding within the lower mantle. We then systematically vary the healing parameters B and η_γ to increase the rheological memory and focus on the results from ∼30 models. All model runs start from a mobile-lid stage and ran for a period of at least 75 overturn times (OT). One OT is defined as the ratio of twice the thickness of the mantle divided by the time average of the root-mean square velocity of the model and corresponds to ∼200 Myr for Earth.

We proceed to discuss surface patterns of the effective viscosity and second strain-rate tensor invariant as well as depth slices of the effective viscosity (Figure 1), to determine the effect of SDWH on convective vigor, surface dynamics and plate reorganizations. To extract quantitative bulk behavior metrics, we focus on time-averages of the surface-averaged effective viscosity $\langle \eta_{\text{surf}}/\eta_0 \rangle$, the relative area of inherited weak zones (IWZs) $\langle A_{\text{ID/HD}} \rangle$, as well as the dominant period T_{dom} of the temporally fluctuations of the total surface heat flux Q_{surf} around the mean. The dominant period of Q_{surf} provides a good first-order description of the cyclicity of plate reorganizations. For the time-averaged metrics we discuss, we calculate the median of the full time series of each model, starting at a minimum time of 20 OT to avoid initial condition effects.

To quantify the intensity of SDWH, we calculated the average lithospheric damage $\langle \gamma_L \rangle$ via the depth-integral of γ along a volumetrically averaged radial profile, considering only the upper TBL normalized by Z_{TBL}. The absolute healing rate at the surface and its temperature-dependence within the upper thermal boundary layer mainly control IWZ dynamics, as might be expected, and $\langle \gamma_L \rangle$ can also capture this behavior to first order. The $\langle \gamma_L \rangle$ metric thus provides a good overall estimate on the effectiveness of SDWH and we use $\langle \gamma_L \rangle$ as the control parameter subsequently.

To assess the spatial extent of IWZs, we define their area, A_{ID}, as zones of high damage but no active deformation:

$$A_{\text{ID}}(t,\phi,\theta) = \frac{\gamma(t,\phi,\theta) > \left(\underline{\underline{\gamma_s}} + 2\sigma_\gamma\right)}{\dot{\varepsilon}_{II}(t,\phi,\theta) < \left(\underline{\underline{\dot{\varepsilon}_{II}}} + \sigma_\varepsilon\right)} \cdot d\theta \cdot d\phi \cdot \cos\left(\frac{\theta\pi}{180}\right) \tag{11}$$

where ϕ and θ are the longitude and colatitude, respectively, $\underline{\underline{\gamma_s}}$ is the median of the surface quasi-strain and σ_γ its standard deviation, and $\underline{\underline{\dot{\varepsilon}_{II}}}$ is the median of the surface strain rate and σ_ε its standard deviation (see Text S3 in Supporting Information S1 for further details). The relative fraction of the area of inherited damage relative to the total high-damage area is defined as:

$$A_{\text{ID/HD}} = \frac{\sum A_{\text{ID}}(t,\phi,\theta)}{A_{\text{HD}}} \tag{12}$$

where A_{HD} is the total high-damage area (i.e., $\gamma(t,\phi,\theta) > (\gamma_s + 2\sigma_\gamma)$). The relative area of IWZs, $A_{\text{ID/HD}}$, quantifies the amount of presently non-deforming lithospheric IWZs relative to the entire, highly deformed areas and the intensity of an IWZ is proportional to γ (Equations 8–10).

In the following, we describe the effect of a SDWH rheology on the convective planform and dynamics, in particular the time-dependence of plate reorganization. We first describe different types of IWZ reactivations which are characteristic features of our models (Figure 1) followed by a description of the global effect of strain weakening and rheological memory.

3. Results

3.1. Reactivation of Inherited Weak Zones

Depending on the longevity of memory (governed by B and η_γ), damage accumulation and preservation can be effective to form IWZs within the lithosphere (cf. Foley and Bercovici, 2014; Landuyt et al., 2008). There is a range of surface healing rates, H_{Surf}, for which no IWZs are formed ($H_{\text{Surf}} > 10^3$). Weak zones are formed, but

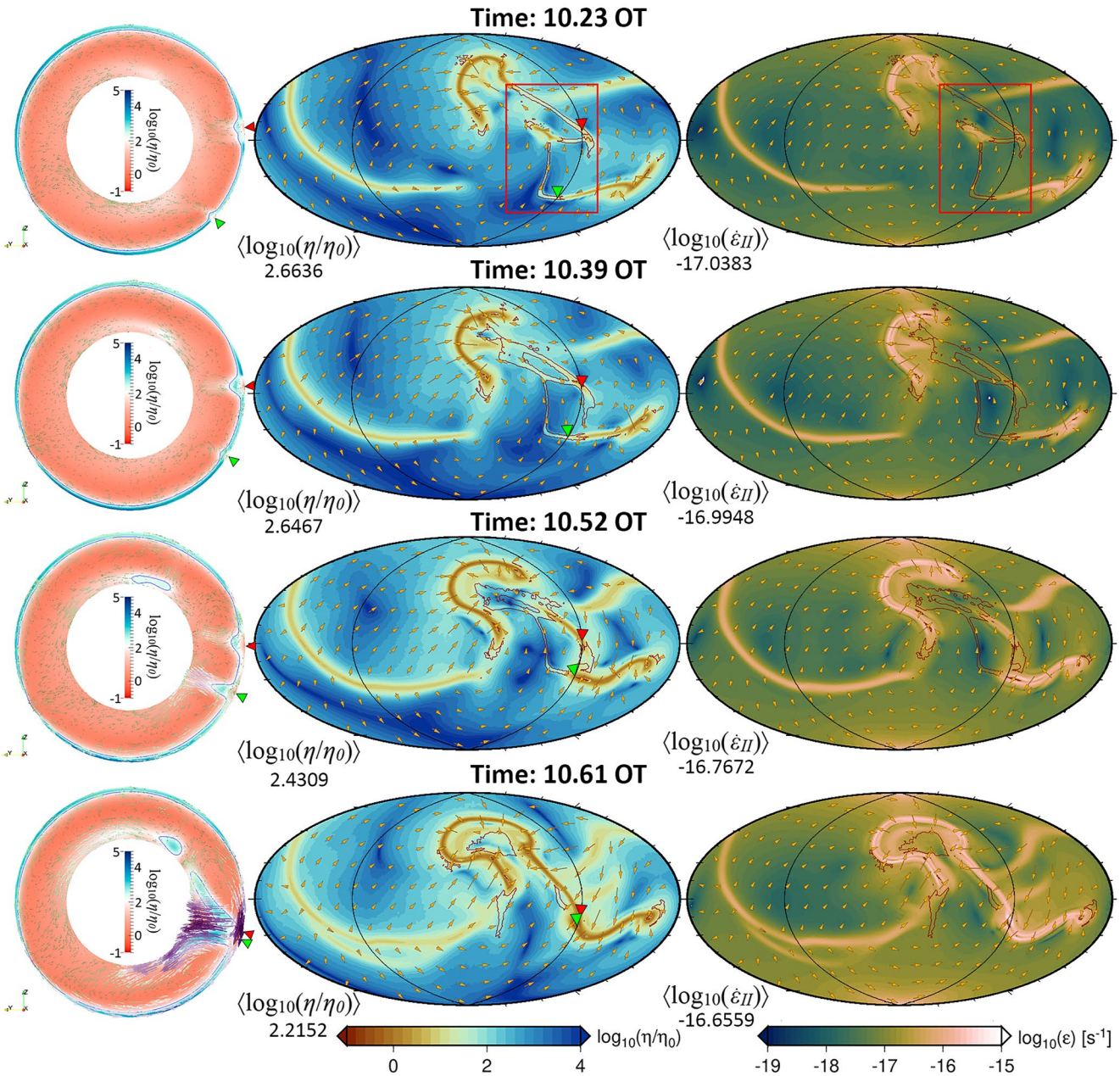

Figure 1. Inherited weak zone reactivation. Snapshots of reactivations of inherited weak zones (IWZs) in a model with strain-dependent weakening parameters of $B = 2.44 \bullet 10^9$ and $\eta_\gamma = 92.103$. Viscosity cross section (left) along the black intersection shown on the surface plots for viscosity (middle) and strain rate (right) with red contours delineating the IWZ area following Equation 12. IWZs can be reactivated in two ways: 1), as guide for a laterally propagating subduction zone (green triangle), and 2), as a newly formed subduction zone (red triangle).

short lived and cannot be reactivated for smaller healing rates ($H_{\text{Surf}} \sim 10^2$–$10^3$). Pronounced IWZ are observed for further reduced rates ($H_{\text{Surf}} = 10^{-1} - 10^3$) in combination with a wide range of temperature-dependence (i.e., a longer memory with depth, e.g., quantifiable via the depth-integral of γ or H). At even smaller $H_{\text{Surf}} \sim 10^{-1} - 10^2$, IWZs can be reactivated, but at the smallest values of $H_{Surf} < 10^{-1}$, lithospheric weakening becomes too intense (see graphic summary in Figure S1 in Supporting Information S1). Introduction of IWZs results in more frequent plate reorganizations due to easier yielding resulting in overall higher convective variability.

Well-pronounced IWZs form due to the continuous deformation along convergent (subduction) zones, enabling a kind of lubrication layer (Figure 1). This becomes apparent once the slab breaks off (highlighted by the dark contour lines in the surface plots). The IWZs are transported laterally with the lithosphere and are then either

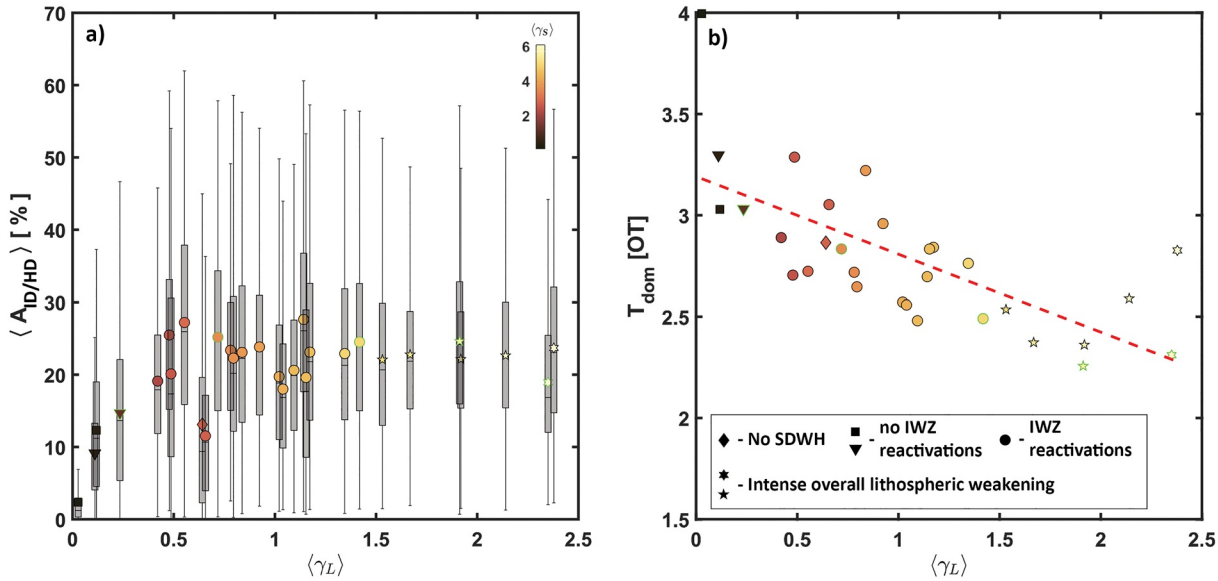

Figure 2. Memory effect and plate reorganization time-dependence. (a) Relative area of inherited weak zones (IWZ); (b) Dominant period of the total surface heat flux Q_{surf}, both shown with symbols showing the median and box whisker plots for the range over model time, against the average lithospheric damage. Symbol color denotes time-averaged surface damage, and the dashed curve a linear fit. Symbol type denotes the reactivation behavior (see text for more details). Symbols with green edge show models from Figure S2 in Supporting Information S1.

subducted along existing convergent boundaries, cut up and dispersed by migrating divergent boundaries, or reactivated as new plate boundaries, both in divergent and convergent margins. This effect is partly controlled by η_γ, as it affects the depth extent of the IWZ. This is similar to earlier findings of 2-D models (e.g., Foley and Bercovici, 2014), including the reactivation behavior explored by Fuchs and Becker (2019). However, a robust quantification of the required weakening intensity as well as depth penetration for reactivation of IWZs is less straightforward for our global models, mainly due to the additional degrees of freedom (lateral and vertical extent of IWZs) provided by 3-D flow.

We can, however, discuss some typical behaviors qualitatively. For pronounced IWZs, two different types of reactivations are observed. Figure 1 shows an example with both types; the initial IWZs are highlighted by the red square in the surface plots. An IWZ may serve as, (a), a lateral guide for propagating convergent boundaries (marked with a green triangle), for example, such that an active subduction zone grows laterally. This kind of reactivation is observed frequently within the models and is facilitated by the lower yield stress within the IWZ with respect to the surrounding lithosphere.

A less frequently observed reactivation is, (b), the formation of a new convergent boundary (marked with a red triangle). Such reactivation happens when the IWZ lies within a plate that is under external compression, such as divergent boundaries around their edges, akin to the setting of, for example, present-day Antarctica. The IWZ has a lower yield stress than the adjacent lithosphere. Due to the increasing thickening of the top thermal boundary layer in a compressional stage, further weakening occurs within the IWZ until a new convergent boundary is formed. In the given example, both newly formed subduction zones happen to connect with each other, a phenomenon that can be observed more frequently in an oceanic-lithosphere-only setting.

Type 2 reactivation results from the interaction of the large-scale plate dynamics, and a well-established IWZ. Reactivation via a new convergent boundary is less frequent than reorganization via lateral propagation. Models with continental lithosphere that is recycled more slowly may make this scenario more likely. IWZs are also reactivated as divergent boundaries. Again, reactivation via a lateral extension of an active boundary (type 1) is observed more frequently than through the formation of a new divergent boundary (type 2).

In case of stronger weakening and longer memory, reorganization happens more frequently due to the, on average, increasingly more weakened lithosphere over the entire model. Such models do not show the type 2 reactivations. Weak zones still serve as guides for laterally propagating subduction zones, but tend to be shorter and, thus, do have a reduced survival rate. A graphic summary of different IWZs reactivation scenarios over the entire range

of parameters explored is shown in Figure S2 in Supporting Information S1, and more detailed time sequences of each reactivation type in Figures S3–S6 in Supporting Information S1.

Based on the reactivation behavior of IWZs, we can assign each model a class with a characteristic convection pattern, surface dynamics, and IWZ reactivation (Figure 2). The first class is defined by models which form IWZs. However, they either harden quickly, or show no reactivation, due to less pronounced IWZs (marked as squares and lower triangles in Figure 2). The second class of models does form distinct IWZs which can be reactivated in type 1 and 2 scenarios (circles). The third class is defined by models with significant overall weakening of the lithosphere; they have short IWZs as well as weak sinking slabs, leading to a more frequent formation and destruction of convergent plate boundaries (pentagrams). The last class of models have intense overall weakening of the lithosphere preventing the formation of IWZs with large strength contrast and thus also have a reduced reactivation ability (hexagrams). Those IWZs tend to be destroyed by subduction instead of being reactivated. This classification correlates with $\langle \gamma_L \rangle$ and thus lithospheric strength which is also predictive for the average surface $\langle \gamma_s \rangle$ (color scale in Figure 2 and Figures S7 and S8 in Supporting Information S1) or the volumetric $\langle \gamma_V \rangle$ damage.

3.2. Damage Weakening and Memory Effect

The classification of reactivation behavior as discussed above is also relevant for other surface metrics (Figure S7 in Supporting Information S1). The effective surface viscosity $\langle \eta_{surf}/\eta_0 \rangle$, for example, is affected by the accumulated damage (Equations 8–10); with increasing memory, $\langle \gamma_L \rangle$ increases, resulting in a linear decrease of $\langle \eta_{surf}/\eta_0 \rangle$. This is due to the shallow lithosphere being continuously at the yielding stress. Once $\langle \gamma_L \rangle$ surpasses ∼45% (equivalent to $\langle \gamma_s \rangle \sim 5$), reactivation switches to a more dynamic behavior. Convective vigor increases as seen from the volumetric and surface RMS velocity increase. Due to such an increased convective vigor and the weakened, laterally more heterogeneous lithosphere, plate reorganization becomes more frequent, eventually leading to more drip-like convection. Our models are in some sense a global perspective of the previous findings of, for example, Foley and Bercovici (2014) based on 2-D models that the ratio of overall damage to healing controls convective vigor. However, we focus on the role and distribution of IWZs and resulting dynamics of the global lithosphere rather than bulk mantle behavior, which may facilitate comparison to plate tectonic metrics and observed styles of plate boundary evolution. The reduction of the effective viscosity contrast between the surface and the interior results in a decrease in plateness and toroidal-poloidal ratio of the surface velocities (Figures S8a and S8b in Supporting Information S1). However, due to a faster convection and thus more effective internal heat transport, the average temperature and mobility decrease (Figures S8c and S8d in Supporting Information S1).

To distinguish between the average and amount of inherited damage within the lithosphere, we determine the relative area of IWZs of the high-damage surface area for each model (Figure 2a). For models with fast hardening and thus not reactivating IWZs, $\langle A_{ID/HD} \rangle$ covers up to 20% of the total high-damage area. The remaining area is described by active plate boundaries. With increasing $\langle \gamma_L \rangle$, the relative amount of IWZ area increases up to ∼40%. That is, more IWZs are formed with potentially higher longevity. However, due to irregularly formed convergent and divergent boundaries, the time variation of $A_{ID/HD}$ remains rather large (∼0%–65%). Over the entire model run there exist shorter periods in which IWZs dominate the high-damage areas and periods with almost no IWZs at all. This feature could be due to our oceanic-lithosphere-only setting, which means continuous recycling of the lithosphere. The presence of more buoyant continental lithosphere would most likely reduce the time variability of $A_{ID/HD}$. However, the overall trend of an increasing area of IWZs should remain, due to frequent breakup and assembly of continental lithosphere.

In our models, we observe an increase in the high-damage area with increasing $\langle \gamma_L \rangle$, but the area of active deformation and IWZs remains ∼ constant. The increase in the high-damage area indicates a more frequent formation of convergent boundaries, due to a faster general yielding. However, the actively deforming area remains ∼ constant, possibly neutralized due to a more frequent slab break off. The latter should result in an increase of the IWZ area, which can only be compensated by a more frequent reactivation of existing IWZs with respect to a low $\langle \gamma_L \rangle$, thus stabilizing the IWZ area. Hence, reactivation dominates over newly formed convergent boundaries or happens at least equally often. An overall damaged lithosphere results in a less effective strength contrast between IWZs and the adjacent lithosphere as well as in less stable slabs, which also limits the high-damage area. In conclusion, the relative IWZ area stagnates and slightly decreases again. For our models, the area of high damage is always less than ∼5% and the area of IWZs is only ∼1.3% of the total surface area.

3.3. Time Dependence of Plate-Reorganizations

The formation and destruction of convergent and divergent boundaries can be quantified by the resulting changes in seafloor age or Q_{Surf}. While the mean Q_{Surf} must equal the internal heat production rate, high temporary fluctuations corresponds to periods in which young seafloor adjacent to divergent boundaries is dominant, akin to the continental drift phase of the Wilson cycle. Low Q_{Surf} indicates relatively older seafloor, or dominance due to convergence, as would perhaps be the case for continent assembly phase. IWZs facilitate more frequent formation of convergent boundaries; this should lead to a decrease in the dominant period of heat flux fluctuations due to the SDWH rheology.

The dominant periods of Q_{Surf} variation (cf. Figure S9 in Supporting Information S1 for details on computation) in our models can capture aspects of such plate-reorganization cyclicity changes (Figure 2b). With an increasing $\langle \gamma_L \rangle$ the dominant period of heat flux variations is indeed found to decrease, meaning that increased memory leads to more frequent plate reorganization (cf. Foley and Bercovici, 2014). The dominant period decreases from ∼3.2 OT (i.e., ∼612 Myr for an average plate velocity of 3 cm/yr) to ∼ 2.3 OT (∼440 Myr) for a model with maximum memory. Such a decreasing trend in the dominant period is also visible in the surface and volumetric velocities, confirming more frequent variation in plate configurations.

A cross correlation analysis between the temporal variability of Q_{Surf} and the IWZ area shows that there is a phase shift corresponding to a delay of ∼0.6 OT. That is, the IWZ area is maximum ∼114 Myr after the maximum in Q_{Surf} (i.e., the divergent boundary dominating period). The delay increases for increasing $\langle \gamma_L \rangle$ up to ∼1.5 OT for a $\langle \gamma_L \rangle = 0.5$ and decreases again toward its mean value of ∼0.6 OT. This highlights that there is an increase in the formation of IWZs due to damage memory in addition to a higher longevity of IWZs. Reactivation as well as stabilization of convergent boundaries (i.e., less frequent formation of new IWZs) reduce the total amount of IWZs which results in a decrease of the correlation with respect to Q_{Surf}.

4. Discussion

The introduction of damage rheology and SDWH in 3-D spherical, quasi plate-like convection models shows that such a memory mechanism indeed leads to inherited zones of persistent weakness. Those affect plate boundary stability, and often, these IWZs are reused for new plate boundaries, similar to what was found by Fuchs and Becker (2019). Reactivation of IWZs for new plate boundaries is well recognized for continental lithosphere (e.g., Buiter & Torsvik, 2014), but may also possibly be a cause for repeatedly developing, oceanic-only retreating subduction zones, like the Australian Tasmanides (e.g., Spencer et al., 2017). Progressively, creation of damaged zones leads to a lithosphere that is more readily broken, and hence more frequent plate reorganizations with a reduction of the dominant periods of heat transport by up to ∼30%.

We assume a constant healing rate which may not be the case in nature. In particular, potentially driven by crustal growth and differentiation, mineralogical transformation (different grain growth rates and weakening abilities), or due to the secular cooling of the planet, the healing rate within the lithosphere and mantle might vary over time (e.g., Foley and Bercovici, 2014). An increase in memory with time, for example, due to increasing amount of continental lithosphere, might result in an increase in $\langle \gamma_L \rangle$, which would lead to an even more frequent plate reorganization and increase in orogenic activity. If healing and damage are controlled by the surface conditions (cf. Foley and Driscoll, 2016), then healing might instead be less variable. Building on work by Foley and Bercovici (2014) and others, it seems promising to further explore the evolution of the distribution of damage zones into thermal evolution models and explore the respective contribution of bulk rheology and lithospheric IWZs and plate boundary evolution.

Before attempting such more complex models, we can speculate about the role of damage for planetary evolution based on our global models. We found that plate tectonics is less stable with damage memory than without. This is consistent with the analysis of Foley and Bercovici (2014), for example, on the role of damage for overall convective vigor, but unlike what might be expected based on strain-localization leading to favored reuse of IWZs. Locally, plate boundaries are indeed found to be relatively longer lived with memory, and the shorter period power in the spectrum of heat loss is somewhat reduced for increasingly damaged models, which implies some damping of fluctuations due to weakening.

However, we did not find robust metrics for documenting the effect of those stabilizing effects on global scales, and the generally high time-variability of any metrics seems to dwarf any trends. The same is true for other bulk

metrics, like toroidal-poloidal ratios, which were comparable across models, and no features such as transform faults arose after inclusion of damage. This might be because we use a moderate viscosity contrast or because our rheological description lacks sufficient weakening. For the parameters explored, the weakening corresponds roughly to a single mineral phase, composite, GSS rheology (Fuchs & Becker, 2021); other damage rheologies, for example, two-phase grain-damage (Bercovici & Ricard, 2016), might behave differently.

Given the limitation of our models, in particular the omission of longer-lived continental lithosphere, we expect that our estimates of the extent of the IWZ saturation area (~20%), and perhaps also the shift in dominant periods of heat transport (~30%), to be underestimates of the actual role of rheological memory for the thermal evolution of the planet. When scaled to Earth, the dominant periods of heat flux are of the same order as those suggested for supercontinental cycles, ~600 Myr (e.g., Condie et al., 2015; Mitchell et al., 2021) though we do, of course, expect feedbacks between continental cover and the cyclicities driven by oceanic lithosphere recycling (e.g., Rolf et al., 2014; Zhong et al., 2007).

It is more meaningful to compare relative changes in cyclicities over Earth's evolution, for example, by considering indications that the supercontinental periodicity has decreased by ~50% since ~2 Ga, and that this was accommodated by an increase in plate speeds and collision frequency (Condie et al., 2015). At face value, such an increase in reorganization speeds is at odds with a simple convective understanding of plate speeds which should scale as $Ra^{2/3}$ implying a reduction due to the decrease in internal heating of perhaps ~30% since 2 Ga. Of course, thermo-chemical convection modifies classic heat flux scalings (e.g., due to water or melting effects, damage and grain-size feedback into rheology, etc.) and convective efficiency and thermal self-regulation of plate tectonics remain debated (e.g., Crowley et al., 2011; Foley and Bercovici, 2014; Korenaga, 2008; Sandu et al., 2011). However, some decrease in convective vigor and hence plate reorganizations over the age of the Earth due to mantle cooling and reduced internal heat production seems plausible. Our results suggest that the generation of an ever more heterogeneous lithosphere may provide a mechanism to counterbalance, and perhaps overcome, the effect of reduced convective vigor over geological time, which may explain, for example, the putative shortening in the supercontinental cyclicity.

5. Conclusions

Global, visco-plastic convection models with damage allow us to improve explorations of the relevance of inherited weak zones for plate reorganization in a dynamically consistent fashion. Reactivation of inherited weak zones for plate reorganizations are well documented for the Cenozoic (e.g., Crameri et al., 2020) and our models show similar reactivation patterns, as well as a ~30% decrease in the dominant period of convective heat transport. When interpreted in terms of the long-term evolution and creation of inherited weak zones during the operation of plate tectonics, this suggest that rheological damage accumulation is contributing to the suggested increase in supercontinental and orogenic frequency since the Proterozoic (Condie et al., 2015). More generally, our models and subsequent refinements will allow deriving statistical descriptions of plate tectonic metrics as linked to internal and surface thermo-mechanical dynamics. Such work should contribute to better plate reconstructions and an enhanced understanding of terrestrial planetary evolution.

Data Availability Statement

The mantle convection code *CitcomS* is available at https://geodynamics.org/resources/citcoms. All model input parameters are given in Tables S1. All model input files as well as the postprocessed data and the MATLAB scripts to reproduce the surface plots and the box whisker plots will be made available as an open access data set via https://doi.org/10.5281/zenodo.6546322.

Acknowledgments
We would like to thank the editor Lucy Flesch and our reviewers Ross N. Mitchell and Andrea Tommasi for their efforts and comments which helped to improve the manuscript. TWB was partially support through NSF EAR 1853856 and 2121666. Surface plots are drawn using the Generic Mapping Tools (GMT, www.soest.hawaii.edu/gmt/), and we use the color maps from Crameri (2018). Open Access funding enabled and organized by Projekt DEAL.

References

Arnould, M., Coltice, N., Flament, N., & Mallard, C. (2020). Plate tectonics and mantle controls on plume dynamics. *Earth and Planetary Science Letters*, *547*, 116439. https://doi.org/10.1016/j.epsl.2020.116439

Behn, M. D., Hirth, G., & Elsenbeck, J. R., II. (2009). Implications of evolution on the seismic structure of the oceanic upper mantle. *Earth and Planetary Science Letters*, *282*(1–4), 178–189. https://doi.org/10.1016/j.epsl.2009.03.014

Bercovici, D. (1993). A simple model of plate generation from mantle flow. *Geophysical Journal International*, *114*(3), 635–650. https://doi.org/10.1111/j.1365-246x.1993.tb06993.x

Bercovici, D., & Ricard, Y. (2016). Grain-damage hysteresis and plate tectonic states. *Physics of the Earth and Planetary Interiors*, *253*, 31–47. https://doi.org/10.1016/j.pepi.2016.01.005

Buiter, S. J., & Torsvik, T. H. (2014). A review of Wilson cycle plate margins: A role for mantle plumes in continental break-up along sutures? *Gondwana Research*, *26*(2), 627–653. https://doi.org/10.1016/j.gr.2014.02.007

Burke, K., Dewey, J. F., & Kidd, W. S. (1977). World distribution of sutures—The sites of former oceans. *Tectonophysics*, *40*(1–2), 69–99. https://doi.org/10.1016/0040-1951(77)90030-0

Condie, K., Pisarevsky, S. A., Korenaga, J., & Gardoll, S. (2015). Is the rate of supercontinent assembly changing with time? *Precambrian Research*, *259*, 278–289. https://doi.org/10.1016/j.precamres.2014.07.015

Crameri, F. (2018). *Scientific colour maps: Perceptually uniform and colour-vision*. Zenodo. https://doi.org/10.5281/zenodo.1243862

Crameri, F., Magni, V., Domeier, M., Shephard, G. E., Chotalia, K., Cooper, G., et al. (2020). A transdisciplinary and community-driven database to unravel subduction zone initiation. *Nature Communications*, *11*(1), 1–14. https://doi.org/10.1038/s41467-020-17522-9

Crowley, J. W., Gérault, M., & O'Connell, R. J. (2011). On the relative influence of heat and water transport on planetary dynamics. *Earth and Planetary Science Letters*, *310*(3–4), 380–388. https://doi.org/10.1016/j.epsl.2011.08.035

Dang, Z., Zhang, N., Li, Z. X., Huang, C., Spencer, C. J., & Liu, Y. (2020). Weak orogenic lithosphere guides the pattern of plume-triggered supercontinent break-up. *Communications Earth and Environment*, *1*(1), 1–11. https://doi.org/10.1038/s43247-020-00052-z

Foley, B. J., & Becker, T. (2009). Generation of plate-like behavior and mantle heterogeneity from a spherical, viscoplastic convection model. *Geochemistry, Geophysics, Geosystems*, *612*(8), 18–25. https://doi.org/10.1029/2009gc002378

Foley, B. J., & Bercovici, D. (2014). Scaling laws for convection with temperature-dependent viscosity and grain-damage. *Geophysical Journal International*, *199*(1), 580–603. https://doi.org/10.1093/gji/ggu275

Foley, B. J., & Driscoll, P. E. (2016). Whole planet coupling between climate, mantle, and core: Implications for rocky planet evolution. *Geochemistry, Geophysics, Geosystems*, *17*(5), 1885–1914. https://doi.org/10.1002/2015gc006210

Fuchs, L., & Becker, T. W. (2019). Role of strain-dependent weakening memory on the style of mantle convection and plate boundary stability. *Geophysical Journal International*, *218*(1), 601–618. https://doi.org/10.1093/gji/ggz167

Fuchs, L., & Becker, T. W. (2021). Deformation memory in the lithosphere: A comparison of damage-dependent weakening and grain-size sensitive rheologies. *Journal of Geophysical Research: Solid Earth*, *126*(1), e2020JB020335. https://doi.org/10.1029/2020JB020335

Gerya, T. V. (2013). Initiation of transform faults at rifted continental margins: 3D petrological-thermomechanical modeling and comparison to the Woodlark Basin. *Petrology*, *21*(6), 550–560. https://doi.org/10.1134/s0869591113060039

Gurnis, M., Zhong, S., & Toth, J. (2000). On the competing roles of fault reactivation and brittle failure in generating plate tectonics from mantle convection. In R. G. M. A. Richards (Ed.), *The history and dynamics of global plate motions* (pp. 73–94). American Geophysical Union.

Hirth, G., & Kohlstedt, D. (2003). Rheology of the upper mantle and the mantle wedge: A view from the experimentalists. *Geophysical monograph-American geophysical union*, *138*, 83–106.

Korenaga, J. (2008). Urey ratio and the structure and evolution of Earth's mantle. *Reviews of Geophysics*, *46*(2), RG2007. https://doi.org/10.1029/2007rg000241

Landuyt, W., Bercovici, D., & Ricard, Y. (2008). Plate generation and two-phase damage theory in a model of mantle convection. *Geophysical Journal International*, *174*(3), 1065–1080. https://doi.org/10.1111/j.1365-246x.2008.03844.x

Langemeyer, S. M., Lowman, J. P., & Tackley, P. J. (2021). Transform offsets occurring along divergent plate boundaries in global mantle convection models. *Communications Earth and environment*, *2*(1), 69. https://doi.org/10.1038/s43247-021-00139-1

Lavier, L., Buck, W., & Poliakov, A. N. (2000). Factors controlling normal fault offset in an ideal brittle layer. *Journal of Geophysical Research: Solid Earth*, *105*(B10), 23431–23442. https://doi.org/10.1029/2000jb900108

Mitchell, R. N., Zhang, N., Salminen, J., Liu, Y., Spencer, C. J., Steinberger, B., et al. (2021). The supercontinent cycle. *Nature Reviews Earth & Environment*, *2*(5), 358–374. https://doi.org/10.1038/s43017-021-00160-0

Montési, L. G. (2013). Fabric development as the key for forming ductile shear zones and enabling plate tectonics. *Journal of Structural Geology*, *50*, 254–266. https://doi.org/10.1016/j.jsg.2012.12.011

Moresi, L. N., & Solomatov, V. (1998). Mantle convection with a brittle lithosphere: Thoughts on the global tectonic styles of the Earth and Venus. *Geophysical Journal International*, *133*(3), 669–682. https://doi.org/10.1046/j.1365-246x.1998.00521.x

Moresi, L. N., & Solomatov, V. S. (1995). Numerical investigation of 2D convection with extremely large viscosity variations. *Physics of Fluids*, *7*(9), 2154–2162. https://doi.org/10.1063/1.868465

Ogawa, M. (2003). Plate-like regime of a numerically modeled thermal convection in a fluid with temperature-pressure-and stress-history-dependent viscosity. *Journal of Geophysical Research*, *108*(B2). https://doi.org/10.1029/2000jb000069

Rolf, T., Coltice, N., & Tackley, P. J. (2014). Statistical cyclicity of the supercontinent cycle. *Geophysical Research Letters*, *41*(7), 2351–2358. https://doi.org/10.1002/2014gl059595

Sandu, C., Lenardic, A., & McGovern, P. (2011). The effects of deep water cycling on planetary thermal evolution. *Journal of Geophysical Research*, *116*(B12), B12404. https://doi.org/10.1029/2011jb008405

Spencer, C. J., Roberts, N. M. W., & Santosh, M. (2017). Growth, destruction, and preservation of Earth's continental crust. *Earth-Science Reviews*, *172*, 87–106. https://doi.org/10.1016/j.earscirev.2017.07.013

Sykes, L. R. (1978). Intraplate seismisity, reactivation of preexisting zones of weakness, alkaline magmatism, and other tectonism postdating continental fragmentation. *Reviews of Geophysics*, *16*(4), 621–688. https://doi.org/10.1029/rg016i004p00621

Tackley, P. J. (2000a). The quest for self-consistent generation of plate tectonics in mantle convection models. *Geophysical Monograph-American Geophysical Union*, *121*, 47–72.

Tackley, P. J. (2000b). Self-consistent generation of tectonics plates in time-dependent, three-dimensional mantle convection simulations: 1. Pseudoplastic yielding. *Geochemistry, Geophysics, Geosystems*, *1*(8). https://doi.org/10.1029/2000gc000043

Tackley, P. J. (2000c). Self-consistent generation of tectonics plates in time-dependent, three-dimensional mantle convection simulations: 2. Strain weakening and asthenosphere. *Geochemistry, Geophysics, Geosystems*, *1*(8), 1026. https://doi.org/10.1029/2000gc000043

Tan, E., Choi, E., Thoutireddy, P., Gurnis, M., & Aivazis, M. (2006). GeoFramework: Coupling multiple models of mantle convection within a computational framework. *Geochemistry, Geophysics, Geosystems*, *7*(6). https://doi.org/10.1029/2005gc001155

Tommasi, A., & Vauchez, A. (2001). Continental rifting parallel to ancient collisional belts: An effect of the mechanical anisotropy of the lithospheric mantle. *Earth and Planetary Science Letters*, *185*(1–2), 199–210. https://doi.org/10.1016/s0012-821x(00)00350-2

Turcotte, D. L., & Oxburgh, E. R. (1967). Finite amplitude convective cells and continental drift. *Journal of Fluid Mechanics*, *28*(1), 29–42. https://doi.org/10.1017/s0022112067001880

van Heck, H. J., & Tackley, P. J. (2008). Planforms of self-consistently generated plates in 3D spherical geometry. *Geophysical Research Letters*, *35*(19), L19312. https://doi.org/10.1029/2008gl035190

Wilson, J. T. (1966). Did the Atlantic close and then re-open? *Nature*, *211*(5050), 676–681. https://doi.org/10.1038/211676a0

Zhong, S., Zhang, N., Li, Z.-X., & Roberts, J. H. (2007). Supercontinent cycles, true polar wander, and very long wavelength mantle convection. *Earth and Planetary Science Letters*, *261*(3–4), 551–564. https://doi.org/10.1016/j.epsl.2007.07.049

Zhong, S., Zuber, M. T., Moresi, L., & Gurnis, M. (2000). Role of temperature-dependent viscosity and surface plates in spherical shell models of mantle convection. *Journal of Geophysical Research*, *105*(B5), 11063–11082. https://doi.org/10.1029/2000jb900003

Reference From the Supporting Information

Rozel, A., Ricard, Y., & Bercovici, D. (2011). A thermodynamically self-consistent damage equation for grain size evolution during dynamic recrystallization. *Geophysical Journal International*, *184*(2), 719–728. https://doi.org/10.1111/j.1365-246x.2010.04875.x